Supplementary Material

The Neanderthal in the karst: first dating, morphometric, and paleogenetic data on the fossil skeleton from Altamura (Italy)

M. Lari[a], F. Di Vincenzo[b], A. Borsato[c], S. Ghirotto[d], M. Micheli[e], C. Balsamo[a], C. Collina[f], G. De Bellis[g], S. Frisia[c], G. Giacobini[h], E. Gigli[a,i], J. C. Hellstrom[k], A. Lannino[a], A. Modi[a], A. Pietrelli[g], E. Pilli[a], A. Profico[b], O. Ramirez[i], E. Rizzi[g], S. Vai[a], D. Venturo[l], M. Piperno[f], C. Lalueza-Fox[i], G. Barbujani[d,a], D. Caramelli[a], and G. Manzi[b]

[a]*Dipartimento Di Biologia, Università di Firenze, via del Proconsolo 12, 50122 Firenze, Italy*

[b]*Dipartimento di Biologia Ambientale, Sapienza Università di Roma, Piazzale Aldo Moro 5, 00185 Roma, Italy*

[c]*School of Environmental and Life Sciences, University of Newcastle, Callaghan 2308, Australia*

[d]*Dipartimento di Scienze della Vita e Biotecnologie, Università di Ferrara, via Luigi Borsari 46, 44121 Ferrara, Italy*

[e]*Dipartimento di Studi Umanistici, Università di Roma Tre, Piazza della Repubblica 10, 00185, Roma, Italy*

[f]*Facoltà di Scienze Umanistiche, Sapienza Università di Roma, Piazzale Aldo Moro 5, 00185, Roma, Italy*

[g]*Istituto di Tecnologie Biomediche, CNR, Via F.lli Cervi 93, 20090 Segrate, Milano, Italy*

[h]*Dipartimento di Neuroscienze, Università di Torino, Corso Massimo d'Azeglio 52, 10126 Torino, Italy*

[i]*Institute of Evolutionary Biology* (*CSIC-UPF), Dr. Aiguader 88, 08003 Barcelona, Spain*

[k]*School of Earth Sciences, the University of Melbourne, Parkville 3010, Australia*

[l]*Soprintendenza per i Beni Archeologici della Puglia, via Duomo 33, 74123 Taranto, Italy*

Contents:

1. Supplementary removal procedures

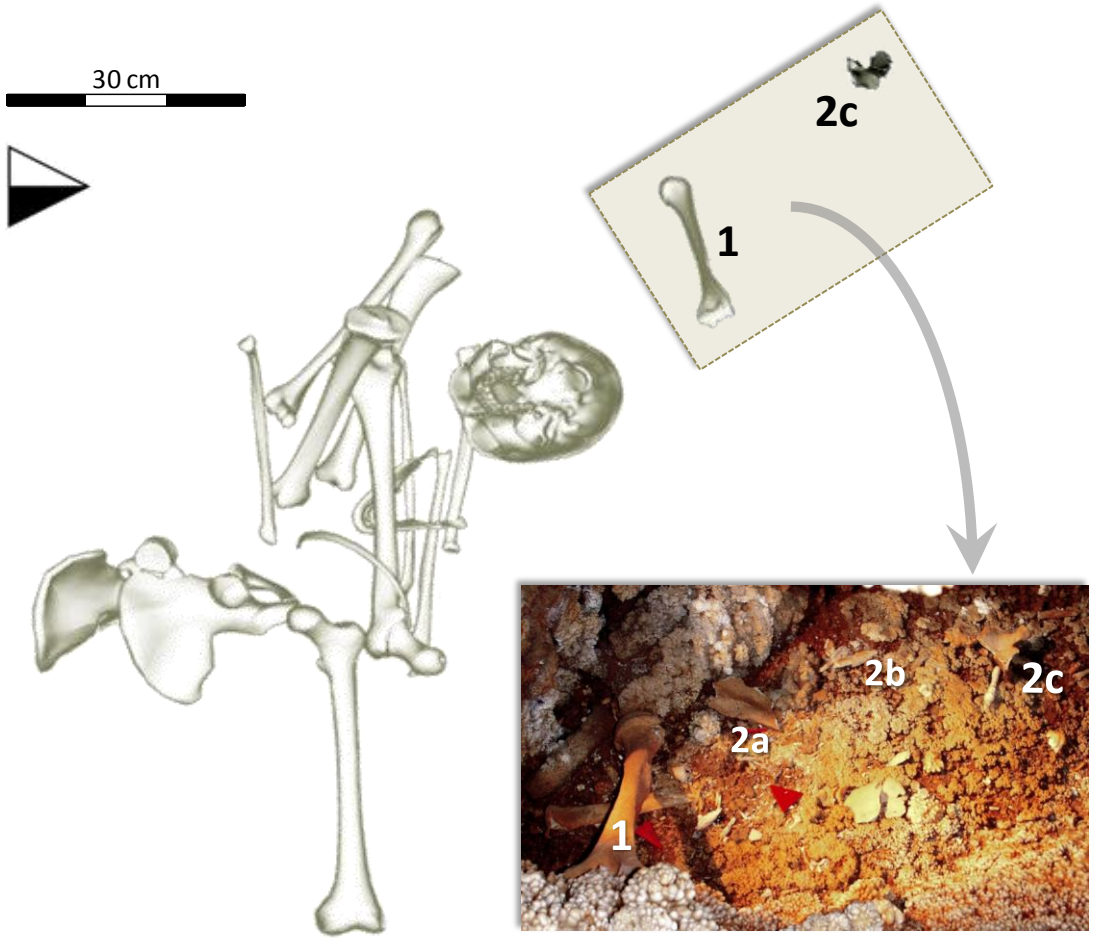

SOM Figure 1. Position of the small chamber (photo) directly behind the area where the main assemblage of bones lies at the end of the so called "ramo dell'uomo" inside the Lamalunga cave of Altamura, Italy. Some bony elements are recognizable: 1) right humerus; 2a) fractured shoulder blade; 2b) other bony fragments; 2c) articular portion of right shoulder (the sample extracted).

The following procedure adopted for the extraction of part of the right scapula (SOM Fig. 1) was inspired by laparoscopic surgery (SOM Fig. 2) as follows:

1. All instruments and other devices were prepared and sterilised on special surgical mats,, including: visual apparatus, consisting of a remote manipulator and a hand-remote controlled instrument in aluminium and carbon fiber with a micro-camera and a high performance halogen light; telemanipulators for extraction, a rod with a manoeuvrable gripping device at the end for immobilizing and extracting the object; sterile plastic bag and refrigerated container;

2. The space directly behind the area of the skeleton was inspected and digital photographic documentation was produced by introducing a remote-controlled digital camera anchored to a support into a slot to the right of the skull (used throughout the operation as the main passage for tools);

3. The sample to be extracted was chosen;

4. The sample was extracted by means of the remotely controlled manoeuvrable gripping device and extraction was photographically recorded;

5. The extracted sample was immediately deposited in a sterile bag and placed inside the refrigerated container.

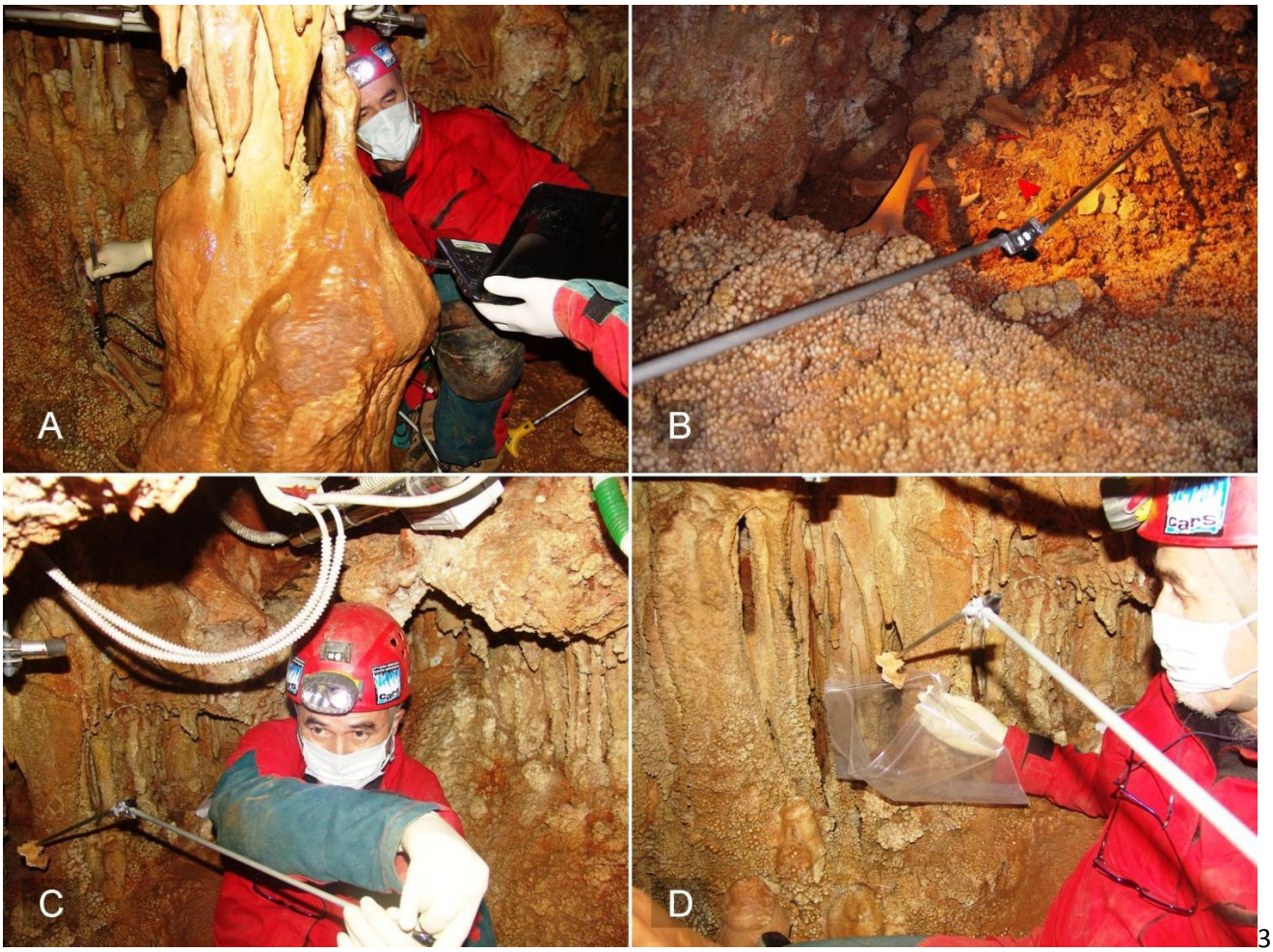

SOM Figure 2. Recovery operations: A) installation of the remote video system designed to allow indirect vision of the surgical scene; B) telemanipulator rod with a manoeuvrable gripping device at the end; C) Extraction of the bone (a portion of the right scapula); D) The bone sample is deposited in a sterile protective bag, still with the use of a device.

2. Supplementary material and methods

a) The sample

The bone sample (SOM Figs. 1, 3) is a portion of the right scapula, broken anteriorly below the inferior border of the scapular glenoid fossa (SGF) and, posteriorly, behind and below the spine. The axillary border is preserved for less than 4.0 mm and the infraglenoid tubercle is positioned on its dorsal edge. Only the base of the acromion process has been preserved and extends dorsally from the spine for a length of less than 3 cm. The supraglenoid tubercle is also present. The notch of the scapula on the superior border is wide (superior width = 19 mm) and appears to be parabolic instead of semicircular. The coracoid process is broken just above the SGF and a wide portion of trabecular bone is exposed. The SGF is well preserved except for the loss of bone along the ventro-caudal border, where the internal spongy bone is visible, and a marked furrow that lies parasagittally 6 mm from the cranial-dorsal rim of the SGF.

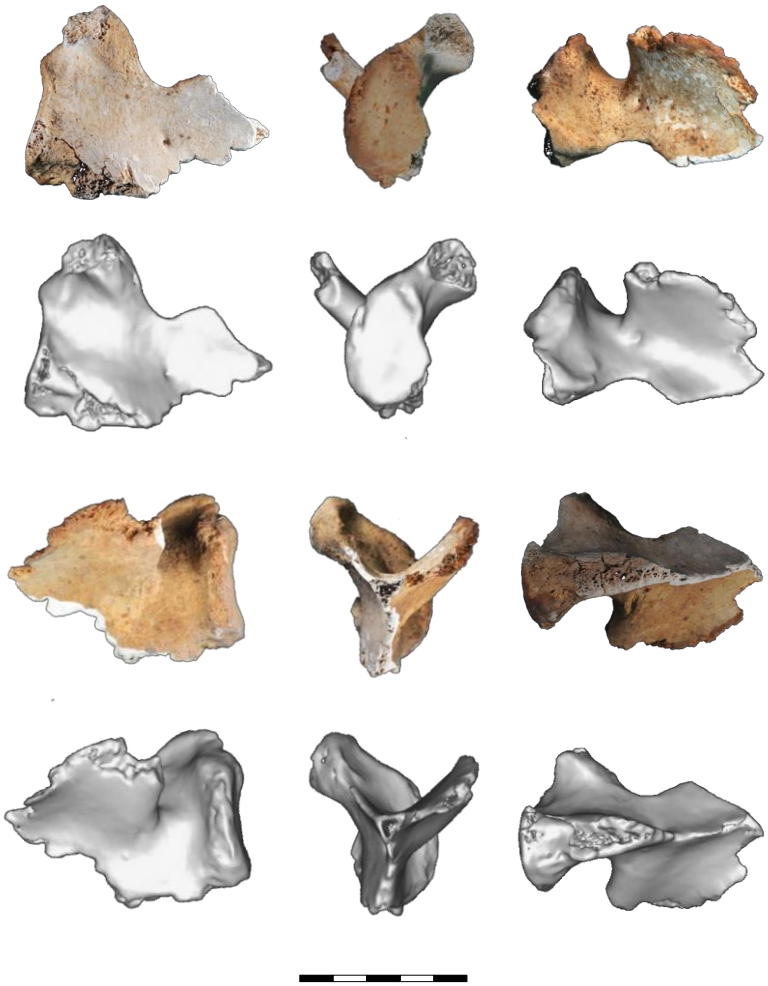

SOM Figure 3. The portion of the right scapula from Altamura compared with its CT-based volume rendering performed on 119 slices in DICOM format with a pixel size of 0.252 mm and slice increment of 0.625 mm. Scale bar = 5 cm.

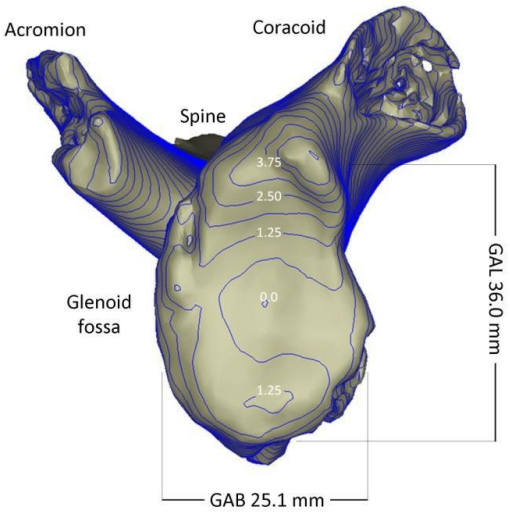

SOM Figure 4. Virtual rendering of the human bone sample from Altamura oriented according to the plane of the scapular glenoid fossa. Metrical variables are reported (GAL, articular length; GAB, articular breadth), while the deepness of the fossa is expressed in mm as isolines from deepest point.

SOM Table 1. List of operational taxonomic units (OTUs) and specimens used for geometric morphometric analyses

OTU	Site	Specimen	Side	Label	Source	Age
Altamura (*n*=1)	Lamalunga Cave (Italy)	Altamura 1	R	Altamura	CT-scan	Late pleistocene
Australopithecus africanus (*n*=1)	Sterkfontein (South Africa)	STS 7	R	STR	Original	Pliocene/Pleistocene
Australopithecus sediba (*n*=1)	Malapa (South Africa)	MH 2	R	MLP	CT-scan	Early Pleistocene
Homo cf. *ergaster* (*n*=1)	Dmanisi (Georgia)	D 4166	R	DMS	CT-scan	Early Pleistocene
Homo floresiensis (*n*=1)	Liang Bua (Flores, Indonesia)	LB 6/4	R	LNG	Original	Late Pleistocene
Homo heidelbergensis (*n*=5)	Atapuerca	AT-320	L	SH1	Original	Middle Pleistocene
	Sima de los Huesos (Spain)	AT-343	L	SH2	Original	Middle Pleistocene
		AT-794	R	SH3	Original	Middle Pleistocene
		AT-1256	R	SH4	Original	Middle Pleistocene
		Atapuerca Scapula 1	R	SH5	Original	Middle Pleistocene
Homo neanderthalensis	Krapina (Croatia)	Krapina 127	R	KR1	Cast	Late Pleistocene
from Krapina (*n*=5)		Krapina 129	R	KR2	Original	Late Pleistocene
		Krapina 130	L	KR3	Cast	Late Pleistocene
		Krapina 131	L	KR4	Original	Late Pleistocene
		Krapina 133	R	KR5	Original	Late Pleistocene
Homo neanderthalensis (*n*=6)	Kebara (Israel)	Kebara 2	R	KBR	Cast	Late Pleistocene
Late European and Near-Eastern samples	La Ferrassie (France)	La Ferrassie 1	R	LF1	Cast	Late Pleistocene
	"	La Ferrassie 2	R	LF2	Cast	Late Pleistocene
	Feldhofer Grotto (Germany)	Neandertal 1	R	NND	Cast	Late Pleistocene
	Shanidar (Iraq)	Shanidar 3	R	SHN	Original	Late Pleistocene
	Tabun (Israel)	Tabun C 1	L	TBN	Cast	Late Pleistocene
Homo neanderthalensis from Vindija (*n*=1)	Vindija Cave (Croatia)	Vi-209	L	VND	Original	Late Pleistocene
Late Pleistocene *Homo sapiens* (*n*=11)	Abri Pataud (France)	Abri Pataud 26 230 A	R	AP	Original	Late Pleistocene
	Dolní Věstonice (Czech Republic)	Dolní Věstonice 3	R	D1	Original	Late Pleistocene
	"	Dolní Věstonice 13	R, L	D2r, l	Original	Late Pleistocene
	"	Dolní Věstonice 14	R, L	D3r, l	Original	Late Pleistocene
	"	Dolní Věstonice 16	L	D4	Original	Late Pleistocene
	Monte Circeo (Italy)	Fossellone 2	L	FS	Original	Late Pleistocene
	Gough's Cave (England)	Gough's Cave 1 118	L	GC	Original	Pleistocene/Holocene
	Bonn-Oberkassel (Germany)	Oberkassel 1	L	O1	Cast	Late Pleistocene
	"	Oberkassel 2	R	O2	Cast	Late Pleistocene
Recent *Homo sapiens*	Strait of Magellan (Chile)	Fuegian 4	R, L	F1r, l	Original	Holocene
Fuegians (*n*=14)		Fuegian 5	R, L	F2 r, l	Original	Holocene
		Fuegian 6	R, L	F3 r, l	Original	Holocene
		Fuegian 7	R, L	F4 r, l	Original	Holocene
		Fuegian 8	R, L	F5 r, l	Original	Holocene
		Fuegian 9	R, L	F6 r, l	Original	Holocene
		Fuegian 13	R, L	F7 r, l	Original	Holocene
Recent *Homo sapiens*	Alfedena (Italy)	Alfedena 126	R, L	A1 r, l	Original	Holocene
Iron Age Italians (*n*=7)		Alfedena 128	L	A2	Original	Holocene
		Alfedena 130	R, L	A3 r, l	Original	Holocene
		Alfedena 132	R, L	A4 r, l	Original	Holocene
Recent *Homo sapiens*	Fezzan (Libya)	Fezzan 3333	L	G1	Original	Holocene
Garamantes (*n*=6)		Fezzan 3334	R, L	G2 r, l	Original	Holocene
		Fezzan 3337	R	G3	Original	Holocene
		Fezzan 3338	L	G4	Original	Holocene
		Fezzan 3347	R	G5	Original	Holocene
Recent *Homo sapiens*	Selvicciola (Italy)	SLV 90 5	R, L	L1 r, l	Original	Holocene
Lombards (*n*=8)		SLV T-84 3	R, L	L2 r, l	Original	Holocene
		SLV T-86 17	R, L	L3 r, l	Original	Holocene
		SLV T-89 8	R, L	L4 r, l	Original	Holocene

b) Morphometrics

Because the specimen was incomplete (particularly owing to the absence of the axillary border), our analyses focused on the morphology of the scapular glenoid fossa (SGF), which was sampled for both traditional and geometric morphometrics.

With regard to traditional morphometrics (SOM Fig. 5), the following variables were selected: GAL, maximum glenoid (articular) length; GAB, maxi- mum glenoid (articular) breadth; GFD, maximum glenoid depth. These measurements were com- pared with data taken from literature relative to the following OTUs: *Australopithecus africanus* (STS 7) [S1], Middle Pleistocene sample from Atapuerca Sima de los Huesos (n = 4) [S2], Late Pleistocene Neanderthals (n = 19), fossils (European Late Pleistocene; n = 5) and recent (n = 99) anatomically modern humans [S3].

As for geometric morphometrics, the analysis was performed on the outline of the glenoid cavity of 68 fossil and recent adult hominins grouped in 10 OTUs (SOM Table 1). Standardized images of each SGF, taken orthogonally to the articular surface, were digitized for analysis by the same single observer (FDV). Images were taken from original specimens, CT scans, or casts (SOM Table 1); to facilitate comparison with the right SGF of Altamura, left isolated specimens and antimeres were mirror imaged before sampling. The outlines were automatically resampled in a configuration of 60 equispaced landmarks using Tps DIG v2.10 (http://life.bio.sunysb.edu/ morph). Following the spline relaxation method [S4,5], we set two points in the configuration to define the tangent direction along which the semilandmarks can slide along the curve with respect to their original position. We used the minimum bending energy criterion (BE) to provide spatial homology between points in the configurations [S4]. Transposed semilandmark raw coordinates were aligned with Procrustes superimposition [S5], which removes information about position and orientation of the configurations and scales each specimen to the same centroid size. The Procrustes shape coordinates were used for the analyses. Missing portions of the Altamura SGF were digitally integrated by TPS based interpolant function. A consensus outline for the SGF of the Neanderthals (n = 12) – whose affinity with Altamura was already suggested by traditional morphemetrics (see SOM Fig. 5) – was superimposed on an iso-oriented image of the Altamura SGF, according to four geometric landmarks. Nevertheless, an analysis performed only with the preserved portion of the outline (data not presented) gave similar results. The measurement error was calculated as per Di Vincenzo and collegues [S6].

c) Paleogenetics

Sample preparation: in the clean-room of the laboratory of Molecular Anthropology at the University of Florence, the portion of the scapula was removed from the sterile plastic bag and, after making photographic documentation under a UV sterilized hood, all the bone surfaces were UV irradiated overnight in a crosslinker. Three small fragments of the bone were subsequently obtained using a sterilized diamond rotating blade at low speed (<10000 rpm), and one fragment was sent directly to the aDNA facility at the Institute of Evolutionary Biology in Barcelona. All of the bone fragments were scraped with a rotating tool to remove a thin external layer and then they were pulverised in a previously sterilized ceramic container (washed first with a 50% bleach solution, then with sterile water, and finally with a 70% ethanol solution, before being UV irradiated overnight). The remaining bone sample was immediately stored at -20°C for further investigations. Globally, three powder aliquots (≈500 mg each) were used for DNA extraction, as described in entry 7 of the Supplementary Bibliography.

PCR amplification of mitochondrial DNA a) At the University of Florence a set of 10 Neanderthal specific primer pairs that cover the entire hypervariable region I (HVR-I) of mitochondrial DNA (mtDNA) [S8] were tested on two microliters of each extract and amplified for 50 cycles, as previously described [S9]. Details of the different primer pairs are reported in SOM Table 2. In order to perform only a panoramic genetic survey of the sample, and to better preserve material for further, more innovative, molecular genetic procedures [S10-S12], only one amplification for each

SOM Table 2. Primers pairs used in this study.

Primers pair name and sequence	*Amplicon length in bp (primers included)*
L15995 CCACCATTAGCACCCAAAG **NH 16132 TACCATAATTACTTGACTACC**	180
L16022 TACCATAATTACTTGACTACC **H16095 TACCATAATTACTTGACTACC**	113
L16106 TACCATAATTACTTGACTACC **H16282 CAAACCTACCCACCCTTACC**	217
NL 16223 CAAACCTACCCACCCTTACC **NH16385 AATAGGGGTCCCTTGACCACCA**	204
L 16299 CCAACAAACCTACCCACCCTTA **NH16400 ATTGATTTCACGGAGGATGG**	143
NL 16311 CCAACAAACCTACCCACCCTTA **H16402 GATTTCACGGAGGATGGTG**	132
NL16,182 AACCTAATCCACATCAACC **NH16,223 TTCAACTGTCATACATCAACTAC**	83
NL16,230 GCACAGCAATCAACCTTCAACTG **NH16,262 TTACACCCACTAGGATATCAACAAACC**	82
NL16,263 CTACAACTCCAAAGACGCCCTTA **NH16,301 CAGTACATAGCACATAAAGT**	81
NL16,220CAAGCAAGCACAGCAATCA **NH16,246 AACTCCAAAGACGCCCTTACA**	66

primer pair was performed on each extract. Globally, 20 PCRs were performed. b) At the Institute of Evolutionary Biology in Barcelona, a two-step PCR protocol was used [S13] to try to amplify the complete HVRI, using a set of nine primers [S14] together with blocking primers, designed to prevent the amplification of possible modern human contaminant DNA [S15].

Cloning and sequencing: at both laboratories, PCR products were cloned using a TOPO TA Cloning Kit (Invitrogen) according to the manufacturer's instructions. Screening of white recombinant colonies was accomplished by PCR as previously reported [S9]. After column purification, 1.5 µl was cycle-sequenced by following the BigDye Terminator kit's (Applied Biosystems) supplier's instructions. The sequence was determined using an Applied BioSystems 3130 DNA Sequencer.

Phylogenetic analysis: all the already available Neanderthal HVRI sequences, the new sequence from Altamura, and the Denisova sequence, were aligned with the CRS [S16] using Clustal X version 2.0 [S17]. The list of specimens included in the analysis, together with their geographical origin and age, are reported in SOM Table 3. Also included in this alignment was the recently published sequence of the hominin from the Sima de los Huesos cave [S18]. In order to explore the evolutionary relationship of all the Neanderthal sequences available with the new sequence from Altamura, we calculated a Neighbor-Joining tree based on the portion of the hypervariable region shared by samples (na-

SOM Table 3. List and details of specimens included in the paleogenetic analyses.

Sequence	*GenBank n.*	*Site*	*Age (BP)*	*Ref.*
CRS	J01415.2	-	-	S16
Vndija75	AF282971	Vindija Cave	> 42,000	S20
Vindija3316	AM948965	Vindija Cave	38,310	S21; S22
Feldhofer2	FM865408	Kleine Feldhofer Grotte	39,240	S23; S10
ElSidron441	DQ859014.2	El Sidron cave	~ 49,000	S24; S14
Feldhofer1	FM865407	Kleine Feldhofer Grotte	39,900	S23; S10
Vindija3325	FM865410	Vindija Cave	~ 38,000	S10
El Sidron1253	FM865409	El Sidron cave	~ 49,000	S10
El Sidron 1240	-	El Sidron cave	~ 49,000	S14
El Sidron 011	-	El Sidron cave	~ 49,000	S14
El Sidron 331c	-	El Sidron cave	~ 49,000	S14
El Sidron 1327h	-	El Sidron cave	~ 49,000	S14
El Sidron 753	-	El Sidron cave	~ 49,000	S14
El Sidron 1161	-	El Sidron cave	~ 49,000	S14
El Sidron 763a	-	El Sidron cave	~ 49,000	S14
El Sidron 566	-	El Sidron cave	~ 49,000	S14
El Sidron 500	-	El Sidron cave	~ 49,000	S14
El Sidron 1634	-	El Sidron cave	~ 49,000	S14
El Sidron 763b	-	El Sidron cave	~ 49,000	S14
El Sidron 634	-	El Sidron cave	~ 49,000	S14
Monti_Lessini	DQ836132	Monti Lessini	~ 50,000	S8
Mezmaiskaya	FM865411	Mezmaiskaya cave	36,300	S25; S10
Okladnikov	EU078680	Okladnikov cave	37,800	S13
Valdegoba	JQ670672	Valdegoba cave	~ 48,500	S26
Teshik-Tash	EU078679	Teshik-Tash	~ 70,000	S13
Scladina	DQ464008	Scladina cave	100,000	S27
Vindija77	-	Vindija Cave		S21
Engis2	-			S21
La Chapelle-aux-Saints	-			S21
Rochers de Villeneuve	-	Les Rochers-de-Villeneuve cave	~ 44,000	S28
Altamura		**Altamura, Lamalunga**		**This study**
Denisova	FN673705	Denisova cave	30,000-48,000	S29
Sima de los Huesos	KF683087.1	Atapuerca, Sima de los Huesos	~ 400,000	S18

mely from 16231 to 16261; see SOM Fig. 6). The Neighbor-Joining tree was constructed with the MEGA 5 software [S19] calculating pairwise distances between sequences, and using Denisova as the outgroup. The robustness of the tree was tested with a standard bootstrap analysis (10,000 replicates).

3. Supplementary results

a) Morphometrics

The deepness of the SGF (2.8 mm) lies within the Neanderthal range reported, respectively, by Churchill and Trinkaus (1990), i.e., 2.6 ± 0.8 mm, and Carretero and collegues (1997), i.e., 2.9 ± 0.9 mm (SOM Fig. 5). This value is far from the modern human condition (3.9 ± 0.7) in Churchill and Trinkaus (1990) and (3.6 ± 0.6 mm) in Carretero and collegues (1997). It also differs from the range of Middle Pleistocene humans from Atapuerca Sima de los Huesos (3.1 ± 0.2 mm) [S2]. By contrast, the SGF of Altamura is not particularly narrow when compared to its length, contrary to the typical Neanderthal condition [S1, S30-32].

As a matter of fact, the glenoid length (GAL) is 36.0 mm and the breadth (GAB) is 25.1 mm, with a breadth/height index of 69.7, which lies at the upper limit of the Neanderthal range (66.0 ± 3.0) and below the modern human range (77.6 ± 3.0) [S2]. The glenoid notch (incisura acetabuli) is deep; thus, the outline of the fossa is not oval, but more pyriform in shape [S30], with the coracoid (i.e., superior) component of the fossa tapering with respect to the wider scapular (i.e., inferior) portion. In this regard, the SGF of Altamura contrasts with the uniformly narrow and cranio-caudally elongated fossae of many Neanderthals.

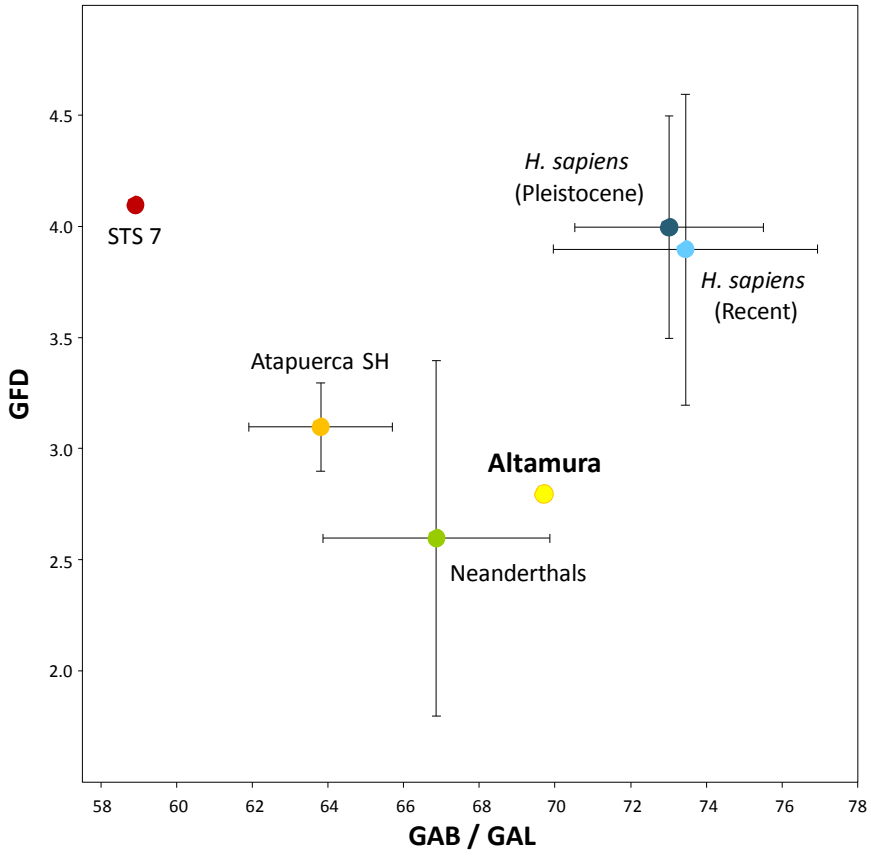

SOM Figure 5. Maximum glenoid fossa depth (GFD) compared to the breadth/height fossa index (GAB/GAL); means and standard deviations are reported. The GFD of the Altamura sample falls within the range of variability of *H. neanderthalensis* and is close to the Atapuerca SH sample (*H. heidelbergensis*). By contrast, while both these samples are characterized by shallow and relatively narrow GFs, when compared to Pleistocene and more recent samples of *H. sapiens*, the Altamura sample shows a somewhat intermediate morphology for this feature (GAB/GAL index).

b) Paleogenetics

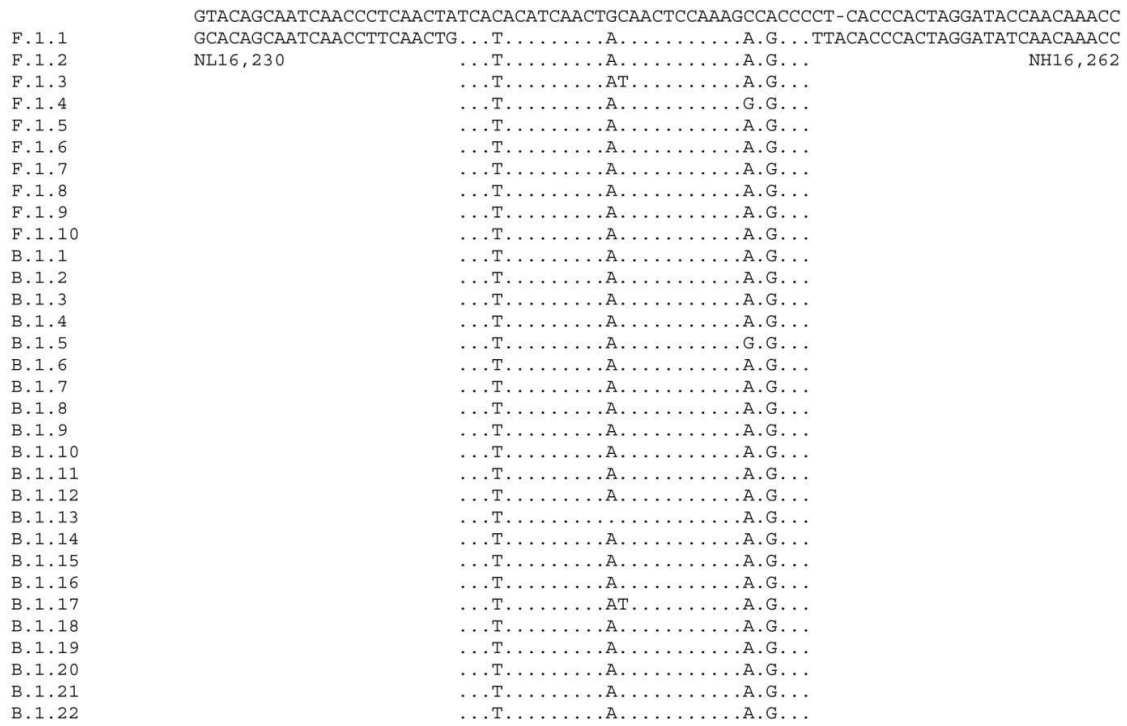

SOM Figure 6. DNA sequences from clones between positions 16,231 and 16261 of mtDNA. The first line reports the reference sequence (CRS). Nucleotides identical to the reference sequence are indicated by dots. Clones are identified by lab codes (F = Florence, B = Barcelona), PCR number relative to each laboratory, and clone number for each PCR.

4. Supplementary references

1. Vrba, E. S., 1979. A new study of the scapula of *Australopithecus africanus* from Sterkfontein. Am. J. Phys. Anthropol. 51, 117—129.
2. Carretero, J.M., Arsuaga, J.L. & Lorenzo, C., 1997. Clavicles, scapulae and humeri from the Sima de los Huesos site (Sierra de Atapuerca, Spain). J. Hum. Evol. 33, 357—408.
3. Churchill, S.E. & Trinkaus, E., 1990. Neandertal scapular glenoid morphology. Am. J. Phys. Anthropol. 83, 147—160.
4. Bookstein, F.L., 1997. Landmark methods for forms without landmarks: morphometrics of group differences in outline shape. Med. Image Anal. 1, 225— 243.
5. Rohlf, F.J. & Slice, D., 1990. Extensions of the Procrustes method for the optimal superimposition of landmarks. Syst. Biol. 39, 40—59.
6. Di Vincenzo, F., Churchill, S.E., Manzi, G., 2012. The Vindija Neanderthal scapular glenoid fossa: Comparative shape analysis suggests evo-devo changes among Neanderthals. J. Hum. Evol. 62, 274—285.
7. Rohland, N., Hofreiter, M., 2007. Ancient DNA extraction from bones and teeth. Nat. Protocols 2, 1756—1762.
8. Caramelli, D., Lalueza-Fox, C., Condemi, S., Longo, L., Milani, L., Manfredini, A., de Saint Pierre, M., Adoni, F., Lari, M., Giunti, P., Ricci, S., Casoli, A., Calafell, F., Mallegni, F., Bertranpetit, J., Stanyon, R., Bertorelle, G. & Barbujani, G., 2006. A highly divergent mtDNA sequence in a Neandertal individual from Italy. Curr. Biol.16, R630—R632.
9. Lari, M., Rizzi, E., Milani, L., Corti, G., Balsamo, C., Vai, S., Catalano, G., Pilli, E., Longo, L., Condemi, S., Giunti, P., Hänni, C., De Bellis, G., Orlando, L., Barbujani, G., Caramelli, D., 2010. The Microcephalin Ancestral Allele in a Neanderthal Individual. PLoS ONE 5, e10648.
10. Briggs, A. W., Good, J.M., Green, R.E., Krause, J., Maricic, T., Stenzel, U., Lalueza-Fox, C., Rudan, P., Brajković, D., Željko, K., Gušić, I., Schmitz, R., Doronichev, V.B., Golovanova, L.V., de la Rasilla, M., Fortea, J., Rosas, A. & Pääbo, S., 2009. Targeted Retrieval and Analysis of Five Neandertal mtDNA Genomes. Science 325, 318—321.
11. Green, R.E., Krause, J., Briggs, A.W., Maricic, T., Stenzel, U., Kircher, M., Patterson, N., Li, H., Zhai, W., Fritz, M. H.Y., Hansen, N. F., Durand, E.Y., Malaspinas, A.S., Jensen, J.D., Marques-Bonet, T., Alkan, C., Prüfer, K., Meyer, M., Burbano, H. A., Good, J.M., Schultz, R., Aximu-Petri, A., Butthof, A., Höber, B., Höffner, B., Siegemund, M., Weihmann, A., Nusbaum, C., Lander, E. S., Russ, C., Novod, N., Affourtit, J., Egholm, M., Verna, C., Rudan, P., Brajkovic, D., Kucan, Ž., Gušic, I., Doronichev, V. B., Golovanova, L. V., Lalueza-Fox, C., de la Rasilla, M., Fortea, J., Rosas, A., Schmitz, R. W., Johnson, P. L. F., Eichler, E. E., Fa— lush, D., Birney, E., Mullikin, J. C., Slatkin, M., Nielsen, R., Kelso, J., Lachmann, M., Reich, D., Pääbo, S., 2010. A Draft Sequence of the Neandertal Genome. Science 328, 710—722.
12. Burbano, H. A., Hodges, E., Green, R. E., Briggs, A.W., Krause, J., Meyer, M., Good, J.M., Maricic, T., Johnson, P. L.F., Xuan, Z., Rooks, M., Bhattacharjee, A., Brizuela, L., Albert, F.W., de la Rasilla, M., Fortea, J., Rosas, A., Lachmann, M., Hannon, G. J., Pääbo, S., 2010. Targeted Investigation of the Neandertal Genome by Array-Based Sequence Capture. Science 328, 723—725.
13. Krause, J., Lalueza-Fox, C., Orlando, L., Enard, W., Green, R.E., Burbano, H.A., Hublin, J.J., Hänni, C. Fortea, J., de la Rasilla, M., Bertranpetit, J., Rosas, A., Pääbo, S., 2007. The Derived FOXP2 Variant of Modern Humans Was Shared with Neandertals. Curr. Biol. 17, 1908—1912.
14. Lalueza-Fox, C., Rosas, A., Estalrrich, A., Gigli, E., Campos, P.F., García-Tabernero, A., García-Vargas, S., Sánchez-Quinto, F., Ramírez, O., Civit, S., Bastir, M., Huguet, R., Santamaría, D., Gilbert, M. T. P., Willerslev, E., de la Rasilla, M., 2011. Genetic evidence for patrilocal mating behavior among Neandertal groups. Proc. Natl. Acad. Sci. USA 108, 250—253.
15. Gigli, E., Rasmussen, M., Civit, S., Rosas, A., de la Rasilla, M., Fortea, J., Gilbert, M.T.P., Willerslev, E., Lalueza-Fox, C., 2009. An improved PCR method for endogenous DNA retrieval in contaminated Neandertal samples based on the use of blocking primers. J. Archaeol. Sci. 36, 2676—2679.
16. Andrews, R.M., Kubacka, I., Chinnery, P.F., Lightowlers, R.N., Turnbull, D.M., Howell, N., 1999. Reanalysis and revision of the Cambridge reference sequence for human mitochondrial DNA. Nat. Genet. 23, 147—147.
17. Larkin, M.A., Blackshields, G., Brown, N.P., Chenna, R., McGettigan, P.A., McWilliam, H., Valentin, F., Wallace, I. M., Wilm, A., Lopez, R., Thompson, J.D., Gibson, T.J., Higgins, D.G., 2007. Clustal W and Clustal X version 2.0. Bioinformatics 23, 2947—2948.
18. Meyer, M., Fu, Q., Aximu-Petri, A., Glocke, I., Nickel, B., Arsuaga, J.L., Martinez, I., Gracia, A., de Castro, J.M.B., Carbonell, E., Pääbo, S., 2013. A mitochondrial genome sequence of a hominin from Sima de los Huesos. Nature 505, 403—406.
19. Tamura, K., Peterson, D., Peterson, N., Stecher, G., Nei, M., Kumar, S., 2011. MEGA5: Molecular

Evolutionary Genetics Analysis Using Maximum Likelihood, Evolutionary Distance, and Maximum Parsimony Methods. Mol. Biol. Evol. 28, 2731—2739.

20. Krings, M., Capelli, C., Tschentscher, F., Geisert, H., Meyer, S., von Haeseler, A., Grossschmidt, K., Possnert, G., Paunovic, M., Pääbo, S., 2000. A view of Neandertal genetic diversity. Nat. Genet. 26, 144—146.
21. Serre, D., Langaney, A., Chech, M., Teschler-Nicola, M., Paunovic, M., Mennecier, P., Hofreiter, M., Possnert, G., Pääbo, S., 2004. No evidence of Neandertal mtDNA contribution to early modern humans. PLoS biology 2, e57.
22. Green, R.E., Malaspinas, A.S., Krause, J., Briggs, A.W., Johnson, P.L.F., Uhler, C., Meyer, M., Good, J.M., Maricic, T., Stenzel, U., Prüfer, K., Siebauer, M., Burbano, H.A., Ronan, M., Rothberg, J.M., Egholm, M., Rudan, P., Brajković, D., Kućan, Z., Gusić, I., Wikström, M., Laakkonen, L., Kelso, J., Slatkin, M., Pääbo, S., 2008. A complete Neandertal mitochondrial genome sequence determined by high-throughput sequencing. Cell 134, 416—426.
23. Schmitz, R.W., Serre, D., Bonani, G., Feine, S., Hillgruber, F., Krainitzki, H., Pääbo, S., Smith, F.H., 2002. The Neandertal type site revisited: interdis— ciplinary investigations of skeletal remains from the Neander Valley, Germany. Proc. Natl. Acad. Sci. U S A 99, 13342—13347.
24. Lalueza-Fox, C., Sampietro, M.L., Caramelli, D., Puder, Y., Lari, M., Calafell, F., Martínez-Maza, C., Bastir, M., Fortea, J., Rasilla, M.D.L., Bertranpetit, J., Rosas, A., 2005. Neandertal Evolutionary Genetics: Mitochondrial DNA Data from the Iberian Peninsula. Mol. Biol. Evol. 22, 1077—1081.
25. Ovchinnikov, I.V., Götherström, A., Romanova, G.P., Kharitonov, V.M., Liden, K., Goodwin, W., 2000. Molecular analysis of Neanderthal DNA from the northern Caucasus. Nature 404, 490—493.
26. Dalén, L., Orlando, L., Shapiro, B., Brandström-Durling, M., Quam, R., Gilbert, M.T.P., Díez Fernández-Lomana, J.C., Willerslev, E., Arsuaga, J.L., Götherström, A., 2012. Partial Genetic Turnover in Neandertals: Continuity in the East and Population Replacement in the West. Mol. Biol. Evol. 29, 1893—1897.
27. Orlando, L., Darlu, P., Toussaint, M., Bonjean, D., Otte, M., Hänni, C., 2006. Revisiting Neandertal diversity with a 100,000 year old mtDNA sequence. Curr. Biol. 16, R400—R402.
28. Beauval, C., Maureille, B., Lacrampe-Cuyaubère, F., Serre, D., Peressinotto, D., Bordes, J.G., Cochard, D., Couchoud, I., Dubrasquet, D., Laroulandie, V., Lenoble, A., Mallye, J.B., Pasty, S., Primault, J., Rohland, N., Pääbo, S., Trinkaus, E., 2005. A late Neandertal femur from Les Rochers-de-Villeneuve, France. Proc. Natl. Acad. Sci. U S A 102, 7085—7090.
29. Krause, J., Fu, Q., Good, J.M., Viola, B., Shunkov, M.V., Derevianko, A.P., Pääbo, S., 2010. The complete mitochondrial DNA genome of an unknown hominin from southern Siberia. Nature 464, 894— 897.
30. Vallois, H.V., 1928. L'omoplate humaine, etude anatomique et anthropologique. Bull. Mem. Soc. Anthropol. Paris 9, 129—168.
31. Stewart, T.D., 1962. Neanderthal scapulae with special attention to the Shanidar Neanderthals from Iraq. Anthropos 57, 779—800.
32. Trinkaus, E., 1983. The Shanidar Neandertals. Academic Press, New York.